ELSEVIER

Journal of Geochemical Exploration 69–70 (2000) 207–211

JOURNAL OF GEOCHEMICAL EXPLORATION

www.elsevier.nl/locate/jgeoexp

Large-scale flow of geofluids at the Dead Sea Rift

H. Gvirtzman[a,*], E. Stanislavsky[b]

[a]*Institute of Earth Sciences, The Hebrew University of Jerusalem, Givat Ram Campus, 91904 Jerusalem, Israel*
[b]*Department of Earth and Planetary Sciences, The Johns Hopkins University, Baltimore, MD, USA*

Abstract

Buoyancy-driven flow associated with salinity variations is proposed as the principal driving force that has caused large-scale migration of brine and hydrocarbons at the Dead Sea Rift. Numerical simulations indicate the coexistence of two basin-scale groundwater flow systems, one atop the other, with opposite flow directions. The first is a density-driven migration of brine through deep aquifers from the rift outward, which has affected hydrocarbon maturation and migration, and the formation of three small gas fields. The second is a topography-driven groundwater flow through relatively shallow aquifers from the surrounding highlands toward the rift valley, which has caused oil biodegradation, forming heavy oils and asphalts. Simulations indicate that flow-field configurations of both groundwater and hydrocarbons have changed during the structural evolution of the rift, illustrating the interrelationships between basin formation, paleohydrology and hydrocarbon reservoir formation.

Keywords: Groundwater; Brine; Hydrocarbons; Rift; Dead Sea; Modeling

1. The Dead Sea Rift

The Dead Sea Rift (Fig. 1), which evolved during the last 15 Ma, is a left-lateral strike-slip transform separating the Sinai–Levant subplate from the Arabian plate (Garfunkel and Ben-Avraham, 1996). The rift includes several en-echelon rhomb-shaped grabens, one of which is the Dead Sea, the lowest land-surface elevations on Earth (−412 m). The Mediterranean Sea invaded the basin at about 3–6 Ma, forming an elongated seawater arm (called Sedom Lagoon), which has evaporated, resulting in the deposition of the thick Sedom Formation evaporites. Since the basin was cut off from the open sea and became a closed basin, a hypersaline lake was formed, in which the fluviatile and lacustrine sediments of the Samra Formation were deposited. The total thickness of the rift's sediment fill is estimated to be 8–10 km.

Mesozoic to Tertiary sediments crop out in the highlands on both sides of the rift valley. The western highlands include a sediment sequence, about 4 km thick, of carbonates, sandstones, marls and chalks, serving as major regional aquifers (Fig. 2A). The groundwater systems on both sides of the rift become separated due to juxtaposition of aquifers on the flanks with aquitards across the faults in the rift valley (Gvirtzman et al., 1997a,b).

2. Brine and hydrocarbon migration

Starinsky (1974) analyzed groundwater samples from deep wells throughout Israel and defined the geochemical characteristics of the Dead Sea Rift-related (R-type) brine. He hypothesized that this brine is a residual product of intensively evaporated

* Corresponding author. Tel.: + 972-2-658-4912; fax: + 972-2-566-2581.
E-mail address: haimg@vms.huji.ac.il (H. Gvirtzman).

0375-6742/00/$ - see front matter
PII: S0375-6742(00)00057-1

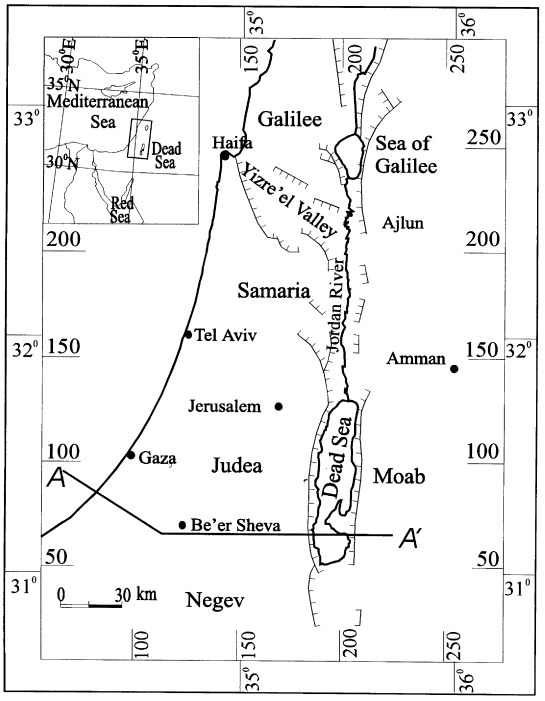

Fig. 1. A map of the studied area showing major faults along the Dead Sea Rift and the location of the geologic cross-section A–A′ (Fig. 2). Map coordinates refer to the Israel grid system.

seawater that invaded the rift, precipitated halite, and later interacted with the host limestone (mainly through dolomitization) during subsurface migration.

The spatial distribution of the R-type brine is not well understood, especially because it is found as far as 100 km away from the rift. The physical feasibility of such long-distance migration, the forces involved, the flow rate, duration, and pathways are unknown. In fact, one should expect a reversed flow direction because during rift–basin formation, topography-driven flow is the dominant flow mechanism, forcing groundwater from the surrounding aquifers toward the deep drainage basin (Person and Garven, 1994).

In addition, a variety of asphalts, light and heavy oils and gas were found in the Dead Sea vicinity, from which only three small gasfields are commercial (Gardosh et al., 1996). Based on geochemical parameters, it is well accepted that the Senonian bituminous chalk and marl rocks, buried in the graben, were the source of all these hydrocarbon shows (Tannenbaum and Aizenshtat, 1985). However, the migration pathway of hydrocarbons from the rift outward, to a distance of 10–15 km westward, has never been clearly explained.

To date, little attention has been given to understanding the paleohydrology of the Dead Sea Rift. This study attempts to fill this gap by presenting mathematical models highlighting the interrelationship between structural evolution, brine migration and hydrocarbon accumulation.

3. Numerical modeling

A detailed geologic cross-section, 5 km deep and 170 km long, that traverses the Mediterranean Sea, the Northern Negev, the Dead Sea, and the Moab Mountains (A–A′ in Fig. 1) was prepared (Fig. 2A). The integrated stratigraphic sequence, which ranges in age from Cambrian to Quaternary, was grouped and divided into various hydrostratigraphic units according to their estimated hydraulic properties. Another geologic cross-section was constructed along the same lines (Fig. 2B) representing the time when deposition of the Sedom Formation had begun and the R-type brine had originated. Several other cross-sections representing intermediate stages were also constructed.

Our approach was to adopt the deformed section as the basis for the hydrodynamic calculations to assess the effects of the structure on fluid migration, salinity redistribution and heat transport across the sedimentary basin. Computations were conducted using the two-dimensional JHU2D code (Garven and Freeze, 1984), which uses the finite-element method to solve the transient fluid and heat flow equations. JHH2D also allows for simulation of separate-phase petroleum and gas migration.

Assignment of material properties (Table 1) for each of the hydrostratigraphic units is based on estimates derived from literature compilations and sensitivity analyses. Longitudinal and transverse dispersivities of 200 and 20 m, respectively, were chosen for all hydrostratigraphic units, which are reasonable for the scale involved. Simulations were conducted for both time periods, 3 and 6 Ma, because of the uncertainty regarding the age of the Sedom Formation, which equals the age of R-type brine and its migration period (Garfunkel and Ben-Avraham, 1996).

Hydraulic boundary conditions are defined by the

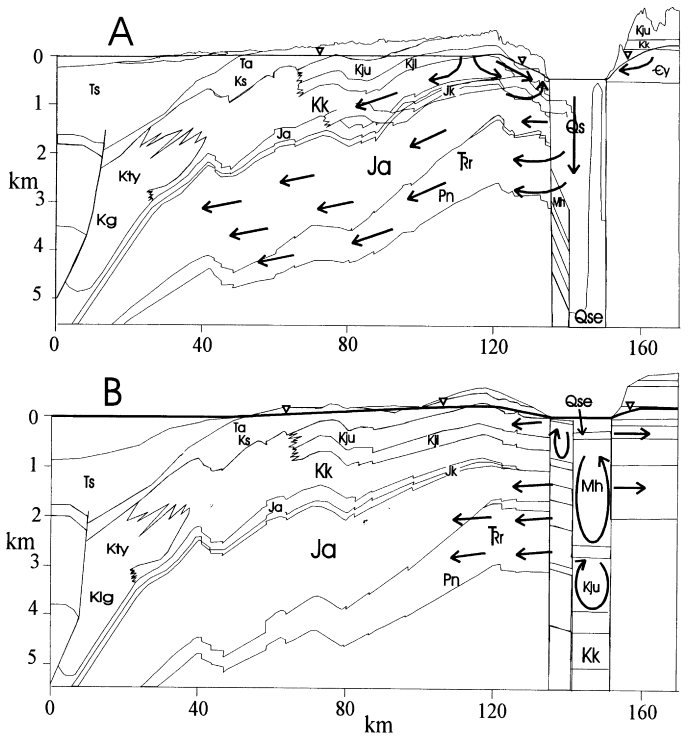

Fig. 2. A geologic cross-section and major flow directions: (A) at present, and (B) at the early Pliocene, illustrating the evolution of the Dead Sea Rift and stages of brine migration. Lithologic symbols are listed in Table 1.

atmospheric pressure at the groundwater table. At the base of the cross-section and at its western and eastern sides, no-flow boundary conditions are assumed (Gvirtzman et al., 1997a). Thermal boundary conditions are defined with a constant temperature of 20°C at the water table, as suggested by a Mediterranean climate. A steady geothermal flux of 45 mW/m^2 is assumed at the bottom boundary. Insulated boundaries have been assumed at both sides of the cross-section. Boundary conditions of water salinity (g of NaCl per 1 g H_2O) were assumed to be 0.0005 g/g at most of the top boundary where rainwater infiltrates the land surface, 0.267 g/g at the Dead Sea, and 0.034 g/g at the Mediterranean Sea. Initial conditions are assumed to be equal to seawater salinity (0.034 g/g) throughout the cross-section.

4. Results and discussion

Once the seawater that had invaded the rift partially evaporated and became more saline, conditions became unstable because heavier water was overlying lighter groundwater. Thus, water penetrated rapidly downward, forming free-convection cells within faulting blocks. Subsequently, a density-driven lateral migration of brine from the basin fill westward was initiated, either in the deep or in the shallow layers, depending on their relative hydraulic permeability.

Once the basin was cut off from the open sea and the lake level dropped, notable hydraulic gradients between the surrounding highlands and the rift valley were formed, which induced local topography-driven flows toward the drainage basin, mainly through shallow aquifers. Consequently, a “flushing” mechanism was initiated with a reversed flow direction, in which the percolating meteoric water at the highlands displaced the previously intruded brine back into the rift.

Stanislavsky and Gvirtzman (1999) postulated the current coexistence of two basin-scale groundwater flow systems, one atop the other with opposite flow

Table 1
Hydrostratigraphic units associated with the geologic cross-section and their physical parameters

Symbols in Fig. 2 and Table 1	Age	Group or Formation	Lithology	Porosity	Regional permeability		
					Bed-parallel hydraulic conductivity (m/yr)[a]	Bed-normal hydraulic conductivity (m/yr)[a]	Thermal conductivity [W/(m °C)]
Qs	Quaternary	Samra Fm.	Marlstone	0.03	1×10^{-2}	1×10^{-3}	2
Qse	Neog.-Quat	Sedom Fm.	Salt	0.01	1×10^{-3}	1×10^{-3}	4
Mh	Miocene	Hazeva Fm.	Sandstone and conglomerate	0.15	8×10^{2}	8×10^{0}	2.5
Ts	Tertiary	Saqiye Gp.	Marlstone	0.03	1×10^{-2}	1×10^{-3}	2
Ta	Tertiary	Avdat Gp.	Chalk and limestone	0.10	1×10^{-1}	1×10^{-3}	2.5
Ks	Cret.-Tert.	Mt. Scopus Gp.	Chalk	0.10	1×10^{-1}	1×10^{-3}	2.5
Kju	Cretaceous	Up. Judea Gp.	Dolomite and limestone	0.15	8×10^{2}	8×10^{0}	2.5
Kjl	Cretaceous	Low. Judea Gp.	Chalk and marl	0.05	6×10^{-1}	6×10^{-3}	2.5
Kty	Cretaceous	Talme Yafe Gp.	Marlstone	0.03	1×10^{-2}	1×10^{-3}	2
Kg	Cretaceous	Gevar'am Gp.	Marlstone	0.03	1×10^{-2}	1×10^{-3}	2
Kk	Cretaceous	Kurnub Gp.	Limestone and sand	0.10	5×10^{0}	5×10^{-2}	2.5
Jk	Jurassic	Kidod Fm.	Marlstone	0.03	1×10^{-2}	1×10^{-3}	2
Ja	Jurassic	Arad Gp.	Carbonates	0.05	1×10^{-1}	1×10^{-3}	2.5
Tr	Triassic	Ramon Gp.	Carbonates	0.05	1×10^{-1}	1×10^{-3}	2.5
Pn	Permian	Negev Gp.	Carbonates	0.05	1×10^{-1}	1×10^{-3}	2.5
-Є y	Cambrian	Yam Suf Gp.	Sandstone	0.15	8×10^{2}	8×10^{0}	2.5
P-Є	Precamb.	Basement	Granite	0	0	0	0

[a] 1 m/year $= 3\times10^{-8}$ m/s $\approx 3\times10^{-15}$ m^2 = 3 mD (millidarcy).

directions (Fig. 2A). The first is a topography-driven groundwater flow from the surrounding highlands toward the rift valley through relatively shallow aquifers (down to about 1 km). The second is a density-driven migration of brine through deeper aquifers (down to 4–5 km) in the opposite direction, from the rift outward.

Particle-tracking simulations were applied also to trace petroleum and gas migration. Computations illustrate that hydrocarbon maturation, migration and accumulation at the Dead Sea Rift were significantly affected by the density-driven groundwater flow.

Once the Mediterranean seawater invaded the rift valley and extensively evaporated, it became much heavier and thus penetrated downward. The descent of cool water and the ascent of hot water in convection cells cooled and heated, respectively, all the surrounding rocks. The normal geothermal gradient was interrupted thereby, and the position of the oil window changed, moving between depths of 2.5 and 4 km.

Once lateral migration started, oil and gas were forced westward with the brine, but with a slightly different flow direction because of their relatively higher viscosity and lower density. Calculations indicate that after 3 My, oil has not been accumulated; rather, dispersed oil droplets are still moving westward at a rate of a few cm per year, either within the Triassic or the Jurassic formations. On the other hand, gas bubbles, which were forced into the rift flanks, have probably been entrapped and accumulated.

Once the basin was cut off from the open sea and its lake level dropped, notable hydraulic gradients between the surrounding highlands and the rift valley were formed. The percolating meteoric water displaced the previously intruded brine back into the rift. Various intensities of meteoric water washing and thereby of biodegradation, have resulted in the removal of saturated and aromatic hydrocarbons from the original oil, forming heavy oils and asphalts (Tannenbaum et al., 1987).

References

Gardosh, M., Kashai, E., Salhov, S., Shulman, H., Tannenbaum, E., 1996. Hydrocarbon exploration in the southern Dead Sea area. In: Niemi, T.N., Ben-Avraham, Z., Gat, J. (Eds.). The Dead Sea, Oxford University Press, Oxford, pp. 57–72.

Garfunkel, Z., Ben-Avraham, Z., 1996. The structure of the Dead Sea Basin. Tectonophysics 266, 155–176.

Garven, G., Freeze, R.A., 1984. Theoretical analysis of the role of groundwater flow in the genesis of stratabound ore deposits, 2. Quantitative results. Am. J. Sci. 284, 1125–1174.

Gvirtzman, H., Garven, G., Gvirtzman, G., 1997a. Thermal anomalies associated with forced and free groundwater convection in the Dead Sea Rift Valley. Geol. Soc. Am. Bull. 109, 1167–1176.

Gvirtzman, H., Garven, G., Gvirtzman, G., 1997b. Hydrogeological modeling of the saline-hot springs at the Sea of Galilee, Israel. Water Resour. Res. 33, 913–926.

Person, M.A., Garven, G., 1994. A sensitivity study of the driving forces on fluid flow during continental-rift basin evolution. Geol. Soc. Am. Bull. 106, 461–475.

Stanislavsky, E., Gvirtzman, H., 1999. Basin-scale migration of continental-rift brines: Paleohydrologic modeling of the Dead Sea basin. Geology 27, 791–794.

Starinsky, A., 1974. Relationship between Ca-chloride brines and sedimentary rocks in Israel. PhD thesis, The Hebrew University of Jerusalem, Israel, 176p (in Hebrew, with English Abstr.).

Tannenbaum, E., Aizenshtat, Z., 1985. Formation of immature asphalt from organic-rich carbonate rock, geochemical correlation. Org. Geochem. 8, 181–192.

Tannenbaum, E., Starinsky, A., Aizenshtat, Z., 1987. Light oils transformation to heavy oils and asphalts—an assessment of the amounts of hydrocarbon removed and the hydrological geological control of the process. Exploration for Heavy Crude Oil and Natural Bitumen, Meyer, R.F. (Ed.). AAPG Stud. Geol. 25, 221–231.